

# A GAN-based dimensionality reduction technique for aerodynamic shape optimization

Jun Zhang (✉ [zhangjun@uestc.edu.cn](mailto:zhangjun@uestc.edu.cn))

University of Electronic Science and Technology of China <https://orcid.org/0000-0002-3516-0392>

Wenzheng Wang

China Aerodynamics Research and Development Center

Qiuyu Wu

University of Electronic Science and Technology of China

Liwei Hu

University of Electronic Science and Technology of China

---

## Research

**Keywords:** aerodynamic shape optimization, generative adversarial network, dimensionality reduction, latent code, curve parameterization

**Posted Date:** August 9th, 2021

**DOI:** <https://doi.org/10.21203/rs.3.rs-754281/v1>

**License:** © ⓘ This work is licensed under a Creative Commons Attribution 4.0 International License.

[Read Full License](#)

---

---

---

# A GAN-based dimensionality reduction technique for aerodynamic shape optimization

Jun ZHANG<sup>1\*</sup>, Wenzheng WANG<sup>2</sup>, Qiuyu WU<sup>1</sup>, Liwei HU<sup>1</sup>

(\*Correspondence: zhangjun@uestc.edu.cn 1. University of Electronic Science and Technology of China, Chengdu 611731, Sichuan, China; 2. China Aerodynamics Research and Development Center, Mianyang 621000, Sichuan, China)

**Abstract:** Aerodynamic shape optimization (ASO) based on computational fluid dynamics simulations is extremely computationally demanding because a search needs to be performed in a high-dimensional design space. One solution to this problem is to reduce the dimensionality of the design space for aircraft optimization. Hence, in this study, a dimensionality reduction technique is designed based on a generative adversarial network (GAN) to facilitate ASO. The novel GAN model is developed by combining the GAN with airfoil curve parameterization and can directly produce realistic and highly accurate airfoil curves from input data of aerodynamic shapes. In addition, the respective interpretable characteristic airfoil variables can be obtained by extracting latent codes with physical meaning, while reducing the dimensionality of the airfoil design space. The results of simulation experiments show that the proposed technique can significantly improve the optimization convergence rate of the ASO process.

**Keywords:** aerodynamic shape optimization; generative adversarial network; dimensionality reduction; latent code; curve parameterization

## 0. Introduction

Aerodynamic shape design is a core technology for aircraft. An excellent aerodynamic shape translates into high aircraft performance. Aerodynamic shape optimization (ASO) is an important step in aerodynamic shape design. An optimum search algorithm can be used to determine the optimum search direction with aerodynamic parameters (e.g., the lift-to-drag ratio ( $C_L/C_D$  ratio) and flight power) as constraints to ensure that the required aerodynamic objective

function is satisfied. The ultimate goal is to find an extreme value for the objective function or a feasible region that meets the design requirements.<sup>[1]</sup>

Computational fluid dynamics (CFD) techniques are playing an increasingly important role in aerodynamic shape analysis and design.<sup>[2]</sup> ASO combines CFD and optimization theories to calculate the extreme value of the objective function, taking advantage of a computer's ability to perform fast computations and multiple iterations, while satisfying

---

About the first author: Jun ZHANG was born in 1972 and is an engineer at the School of Computer Science and Engineering of the University of Electronic Science and Technology of China. He has had a long career in teaching and research in the fields of computer software, network communication, and machine learning.

the required aerodynamic conditions to produce high-performance aerodynamic shape designs. Conventional ASO methods based on gradients<sup>[3][4]</sup> and genetic algorithms<sup>[5][6]</sup> often require relatively large design spaces and are therefore associated with enormous iteration-related computational loads. By contrast, global optimization methods based on surrogate models<sup>[7–10]</sup> reduce the number of simulation iterations through downsampling the sample space and using an model to approximate the original objective function. However, these methods also produce an exponential increase in the computational load with the dimensionality of the design variables. One solution to the problem of high-dimensional design variables involved in aerodynamic shapes is to reduce the dimensionality of the design space and extract characteristic variables, thereby improving upon optimization methods based on surrogate models.<sup>[11–16]</sup> Two types of methods are currently mainly used to implement this solution, namely, dimensionality reduction (DR) methods based on linear techniques<sup>[17]</sup> and nonlinear methods based on artificial neural networks.

The rapid development of neural networks and deep learning technology in recent years has produced a novel approach for implementing ASO that has garnered considerable attention from the academic community. Dimensionality reduction has been extensively investigated in the deep learning field. Deep neural network algorithms, such as variational

autoencoders<sup>[18]</sup> and generative adversarial networks (GANs),<sup>[19]</sup> have been found to successfully represent data in complex, high-dimensional distributions (e.g., images) through low-dimensional latent codes (LCs). These techniques based on deep learning can effectively reduce data complexity and maximize the integrity of effective information, while achieving data dimensionality reduction.

Hennigh proposed Lat-Net,<sup>[20]</sup> in which deep neural networks compress the computational time and memory cost of lattice Boltzmann flow simulations. Lat-Net uses convolutional autoencoders and fully differentiable residual connections to compress the state size of a simulation and learns the dynamic results of the compressed form. Once trained, Lat-Net can be extended to large grids and complex geometries, without a loss of accuracy. Achour and Sung et al. successfully used a conditional GAN (CGAN) to reduce the dimensionality of an airfoil design space.<sup>[21]</sup> The CGAN trains on data labels and can generate aerodynamic shape data with any given labels. Labeling each airfoil with precomputed aerodynamic characteristics (e.g., the  $C_L/C_D$  ratio and structural requirements) can be used to guide the shape generation process towards labeled samples of particular types. Thus, the CGAN constitutes novel strategy for shape optimization.

## 1. Model structure

The basic concept of dimensionality reduction is to convert high-dimensional data to low-dimensional

representations. Dimensionality reduction improves the data-processing speed by preserving some of the most important features of high-dimensional data while removing noise and unimportant features. The most notable feature of the encoder-decoder model structure used in the deep learning field is the presence of an intermediate layer, i.e., an intermediate code for data. If the dimensionality of the intermediate layer is lower than that of the original data, the intermediate code is a reduced-dimensional representation of the original data that can be restored to the original data through the decoder.

### 1.1 BézierGAN

The GAN used in this study, BézierGAN, is a dimensionality reduction model with an encoder-decoder structure.<sup>[22]</sup> The BézierGAN adopts the basic structure of the interpretable representation learning using an information maximizing GAN (InfoGAN)<sup>[23]</sup> and can map the probability model of the original data to several specific LCs, each of which represents one feature of the original data. Therefore, the BézierGAN can reduce the dimensionality of the original data at the feature level.

The BézierGAN model structure primarily differs from that of the InfoGAN by a Bézier layer constructed in the output part of the encoder for producing the parameters of the Bézier curve equation. The Bézier layer is constructed because discrete point sets for airfoil curves generated by conventional GANs cannot effectively represent some basic curve properties (e.g.,

smoothness and continuity), which are often better represented and controlled by the parametric equations of curves (e.g., Bézier or spline curves).

### 1.2 Network architecture

Figure 1 shows the BézierGAN architecture, which consists of a generator and a discriminator.

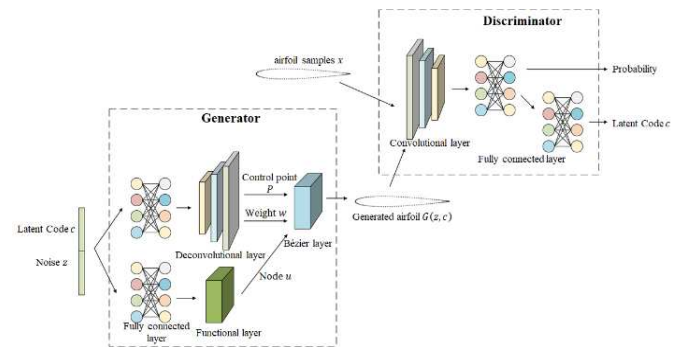


Figure 1. BézierGAN architecture

#### (1) Discriminator

The input of the discriminator is the two-dimensional coordinate vector  $x$  of the discrete points on the continuous airfoil curve. The discriminator outputs two terms, namely, the probability that the data originate from real samples and the predicted LC.

#### (2) Generator

The generator converts the input LC and noise to a control point  $P$ , a weight  $w$ , and a node variable  $u$  for the Bézier curve. The Bézier layer subsequently converts these Bézier parameters to discrete points on the airfoil curve, forming the final airfoil curve pattern. The generator combines the input LC  $c$  and noise  $z$  in the first layer of the network, forming an independent vector  $cz$  that then propagates forward along two different paths. On one path,  $cz$  first passes through two fully connected neural networks, followed by three deconvolutional layers, and eventually outputs a control point  $P$  and a weight  $w$  for the Bézier curve, each

through an independent convolutional layer. On the other path,  $cz$  passes through three fully connected layers in which computations are performed and then produces a node variable  $u$  for the Bézier curve following a simple transformation through a functional layer.

### 1.3 Bézier layer

After the network outputs the learned Bézier parameters (i.e.,  $P$ ,  $w$ , and  $u$ ), the Bézier layer converts these parameters to a coordinate point  $x$  on the discrete airfoil curve using the function given in Equation (1):

$$X_j = \frac{\sum_{i=0}^n \binom{n}{i} u_j^i (1-u_j)^{n-i} P_i w_i}{\sum_{i=0}^n \binom{n}{i} u_j^i (1-u_j)^{n-i} w_i}, j = 0, \dots, m \quad (1)$$

where  $n$  is the order of the Bézier curve and  $m + 1$  is the number of discrete nodes on the curve. Because the  $P$ ,  $w$ , and  $u$  parameters in the equation are differentiable, the network can be trained using the backpropagation algorithm.

### 1.4 Regularization terms

To prevent BézierGAN from converging to a relatively inferior local optimal solution, regularization terms can be used to adjust the abovementioned Bézier parameters.

#### (1) Weight

L1 regularization can be applied to the weight to eliminate the effects of unnecessary or extreme control points, thereby minimizing the number of redundant control points.

$$R_1(G) = \frac{1}{N_n} \sum_{j=1}^N \sum_{i=0}^n |w_i^{(j)}| \quad (2)$$

#### (2) Control points

The dispersiveness and randomness of the control points may cause anomalous behavior of the weight and node variables. Regularization can be used to reduce the distance between control points. The mean and maximum Euclidean distances between two adjacent

control points are used as the regularization term in Equations (3) and (4), respectively:

$$R_2(G) = \frac{1}{N_n} \sum_{j=1}^N \sum_{i=1}^n \|P_i^{(j)} - P_{i-1}^{(j)}\| \quad (3)$$

$$R_3(G) = \frac{1}{N} \sum_{j=1}^N \max_i \{ \|P_i^{(j)} - P_{i-1}^{(j)}\| \} \quad (4)$$

where  $N$  is the sample size.

## 2. Correlation analysis method for LCs

The correlations between the LCs and the physical characteristics of the airfoil are analyzed to examine the interpretability of the dimensionality reduction model.

### 2.1 Correlation evaluation metric

In this study, the linear regression and determination coefficient  $R^2$  is primarily used to evaluate the correlations between the LCs and the physical characteristics of the airfoil (i.e., the radius of the leading edge  $R_l$ , the thickness of the trailing edge  $H_t$ , the maximum thickness  $H_{\max}$ , and the maximum camber  $C_{\max}$ ).

### 2.2 Correlation analysis algorithm

The LC vector  $\vec{c}$  is uniformly sampled in the domain of the function. Figure 2 shows the airfoil curves generated using different values of  $\vec{c}$ . These generated airfoils are arranged in ascending order of the value of each LC component  $c_i$ .

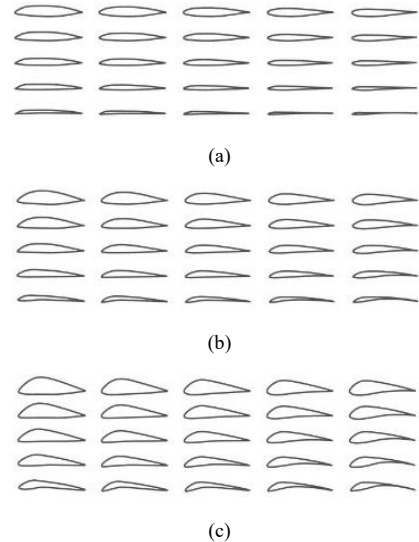


Figure 2. Examples of variations in the airfoil with the code

The control variable algorithm is used to analyze the correlations between the LCs and airfoil characteristics using the procedure given below.

(1) Sample the component  $c_i$  of the LC vector  $\vec{c}$  once at  $1/n$  intervals in the range of  $[0, 1]$ , while maintaining the numerical values of the other components of  $\vec{c}$  unchanged.

(2) Input  $\vec{c}$  into the dimensionality reduction model to produce airfoil data with a sample size  $n$ .

(3) Calculate the physical parameters based on each of the  $n$  airfoil data points using Profili software.

(4) Determine the characteristic physical parameters of the airfoil and find the physical parameter  $p$  that best matches the  $i^{\text{th}}$  dimension  $c_i$  of the LC.

(5) Evaluate the correlation between  $c_i$  and  $p$  and draw a conclusion.

### 3. LC-based ASO

The essence of the ASO process is the solution of the equation

$$\mathbf{x}^* = \underset{\mathbf{x}}{\operatorname{argmin}} f(\mathbf{x}) \quad (5)$$

where the variable  $\mathbf{x}$  represents an aerodynamic airfoil design (in the experiments conducted in this study,  $\mathbf{x}$  is either the LC  $c$  of the BézierGAN or a principal components analysis (PCA)<sup>[24]</sup> or the parameter of the nonuniform rational basis spline (NURBS) equation) and  $f(\mathbf{x})$  is the evaluation function for the aerodynamic properties of the aircraft defined in  $\mathbf{x}$ . Therefore, finding an optimum shape  $\mathbf{x}^*$  is equivalent to finding an optimum LC  $c^*$ . Thus, the optimization problem in Equation (5) is transformed to solving Equation (6).

$$\mathbf{c}^* = \underset{\mathbf{c}}{\operatorname{argmin}} h(\mathbf{c}) = f(\mathbb{E}_{\mathbf{z} \sim P_{\mathbf{z}}} [G(\mathbf{c}, \mathbf{z})]) \quad (6)$$

Then,  $\mathbf{c}^*$  is used to generate an optimum aerodynamic shape  $\mathbf{x}^* = G(\mathbf{c}^*, \mathbf{z})$ .

Bayesian optimization<sup>[25]</sup> is performed to search for  $\mathbf{c}^*$ . It has two components, namely, a priori model and an acquisition function. In this study, efficient global optimization (EGO)<sup>[26]</sup> is employed to implement Bayesian optimization. In EGO, Gaussian process regression (GPR) and expected improvement (EI) are used as the priori model and acquisition function, respectively.

$$\mathbb{E}[I(\mathbf{c})] = \mathbb{E}[\max(h_{\min} - h(\mathbf{c}), 0)] \quad (7)$$

In the equation above,  $h_{\min}$  is the optimal value of the current function. In each step  $t$  of EGO, the  $\mathbf{c}^{(t)}$  that best optimizes the current optimal solution is sought:

$$\mathbf{c}^{(t)} = \underset{\mathbf{c}}{\operatorname{argmax}} \mathbb{E}[I(\mathbf{c})] \quad (8)$$

The EGO procedure is described below.

(1) Estimate the function  $h$  using the GPR.

(2) Calculate the EI using Equation (7) and the learned GPR model.

(3) Search for point  $\mathbf{c}^{(t)}$  with the maximum EI value (i.e., solve Equation (8)).

(4) Evaluate  $h$  at  $\mathbf{c}^{(t)}$  and add a new  $(\mathbf{c}^{(t)}, h(\mathbf{c}^{(t)}))$  pair to the dataset to learn the GPR.

## 4. Experiments and analysis of results

### 4.1 Experimental dataset

Experiments were performed on the airfoil dataset produced by the University of Illinois Urbana-Champaign (UIUC). This dataset contains approximately 1500 airfoil coordinate files in a .dat format.

Here, the NACA 0012 airfoil is used as an example.

Figure 3(a) shows an example of the content of the NACA 0012 airfoil file. The first row shows the name of the airfoil. The left and right columns show the  $x$ - and  $y$ -axis coordinates, respectively. These coordinates form the upper and lower surfaces of the airfoil. Figure 3(b) shows an airfoil graph corresponding to the coordinate file.

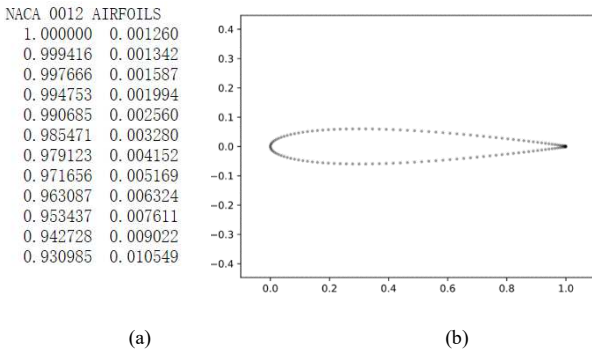


Figure 3. An example of UIUC airfoil data

## 4.2 Dimensionality reduction experiments

In this experiment, PCA — the most commonly used DDR method in the machine learning and statistical fields — was used as a reference to measure and evaluate the performance of the GAN-based technique in reducing the dimensionality of aerodynamic shape data.

### 4.2.1 Data evaluation metrics

(1) Mean log-likelihood (MLL). This metric is commonly used to evaluate generative models. A high MLL indicates a high similarity between generated and real data in terms of the distribution.

(2) Smoothness. The relative variance of differences (RVOD) was used to measure the relative smoothness between the generated discrete coordinate points and the coordinate points in the dataset.

(3) Latent space consistency (LSC). This metric is a measure of the regularity of the latent space. A high LSC indicates that the shape varies consistently along any direction in the latent space.

### 4.2.2 PCA-based dimensionality reduction

The statistical metrics in Tables 1 and 2 and the graphs in Figures 4 and 5 show that the PCA-based method also reduced the dimensionality of the aerodynamic shape data but was outperformed by the BézierGAN-based method in terms of the metrics.

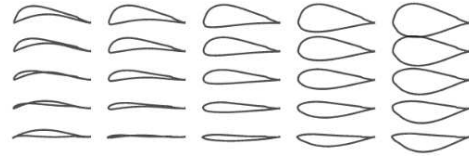


Figure 4. PCA-generated airfoils

Table 1. Evaluation metrics for PCA-based DR

MLL	LSC	Smoothness
691.2	0.079	1.005

### 4.2.3 BézierGAN-based dimensionality reduction

Figure 5 shows the airfoils generated by the BézierGAN model after 20,000 times of training. Thus, these airfoils meet the requirements.

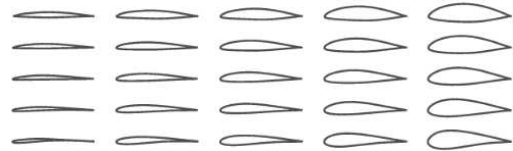


Figure 5. Airfoils generated by the BézierGAN model

Table 2. Evaluation metrics for BézierGAN-based DR

MLL	LSC	Smoothness
947.0	0.986	0.943

### 4.2.4 LC analysis

#### (1) LC design

Inputting a set of preset LCs into a trained BézierGAN model generates a corresponding airfoil curve. In this study, we choose to sample LCs in a

uniformly distributed manner. Specifically, an LC is sampled once at intervals of 0.25 in the range of  $[0, 1]$ . That is, the domain of the function in one dimension for the LC vector  $\vec{c} = \{c_1, c_2, \dots, c_m\}$  is  $c_i \in \{0.00, 0.25, 0.50, 0.75, 1.00\}$ ,  $1 \leq i \leq m$ . In this experiment,  $m$  was set to 3. Therefore, 125 airfoils were generated.

## (2) Generated airfoil graphs

Figure 6 shows the 125 airfoil curves. The  $x$ - and  $y$ -axes represent the first and second dimensions ( $c_1$  and  $c_2$ , respectively) of the LC vector  $\vec{c} = \{c_1, c_2, c_3\}$ , respectively. The third dimension  $c_3$  varies for the five sets of airfoils shown.

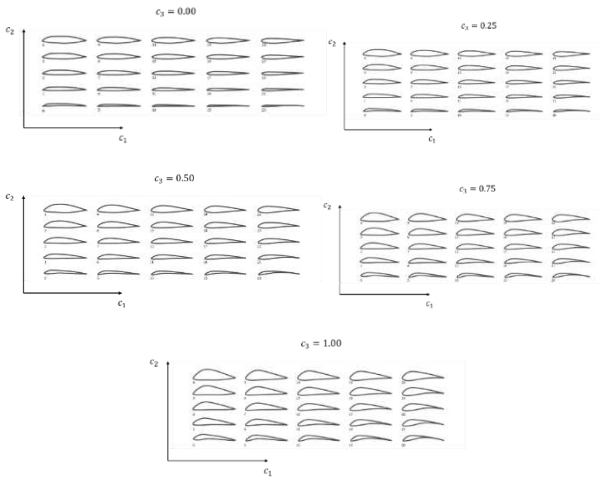
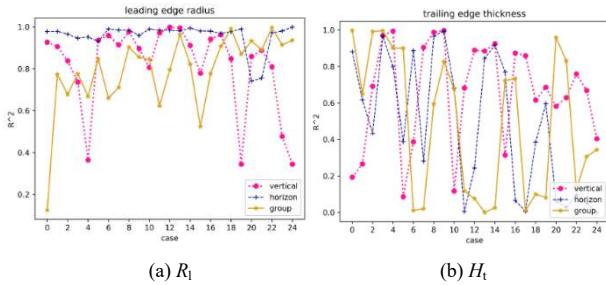


Figure 6. Variation in the airfoil with the LC

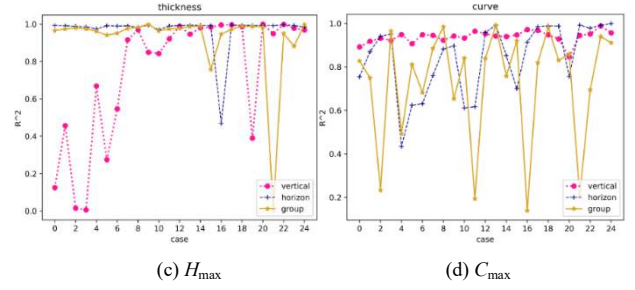
## (3) Correlation analysis

The  $R^2$  values between  $c_1$ ,  $c_2$ , and  $c_3$  and each physical characteristic were extracted and plotted on a single graph for analysis, which is shown in Figure 7.



(a)  $R_l$

(b)  $H_t$



(c)  $H_{max}$

(d)  $C_{max}$

Figure 7. Fitting of each physical characteristic to each LC dimension

Figure 7(a) shows that  $R_l$  was most significantly linearly correlated with the LC in the horizontal direction,  $c_1$ . Figure 7(b) shows that the linear correlation between  $H_t$  and each LC was unstable with a large variance. As a result, the LC that was correlated with  $H_t$  could not be determined. Figure 7(c) shows that  $H_{max}$  was also most significantly linearly correlated with  $c_1$ . As both  $R_l$  and  $H_{max}$  exhibited similarly strong linear correlations with  $c_1$ , it can be inferred that the two characteristics were not independent and affected each other. Figure 7(d) shows that  $C_{max}$  was most significantly linearly correlated with LC in the vertical direction,  $c_2$ . As in Figure 7(b), no correlation was found between  $H_t$  and any LC dimension.

## 4.3 ASO comparative analysis

The PCA- and BézierGAN-based methods for reducing the dimensionality of aerodynamic shape data and the NURBS-based airfoil parameterization method<sup>[27]</sup> were experimentally compared in terms of the iterative optimization process in the EGO algorithm. The main constraints used in the optimization experiments were a Reynolds number of 1,800,000, a Mach number of 0.01 and an angle of attack of  $0^\circ$ . Figure 8 shows the optimization process, that is, the variation in the target  $C_L/C_D$  ratio with the number of

optimization iterations. Table 3 is a summary of the specifications of the ASO experiments and the final  $C_L/C_D$  ratio.

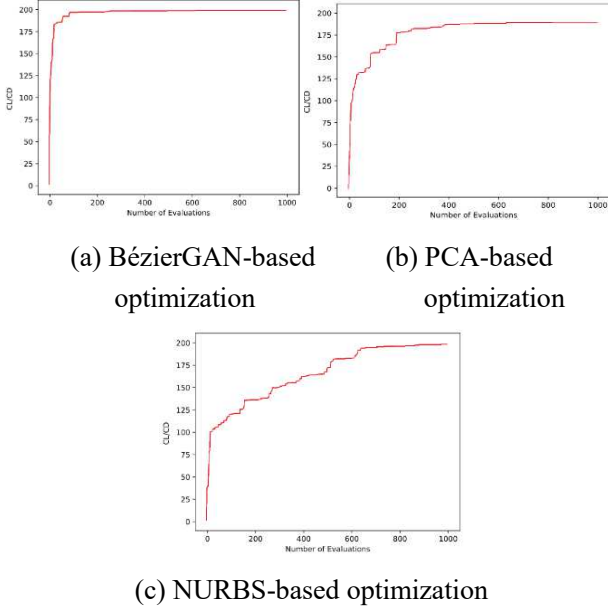


Figure 8. ASO process using three methods

Table 3. ASO results

Curve representation	Iterations	Number of experiments	$C_L/C_D$ ratio
BézierGAN	1000	10	199.3
PCA	1000	10	186.9
NURBS	1000	10	197.2

Figure 8(a) shows that the BézierGAN-based dimensionality reduction method for aerodynamic shape data yielded the required  $C_L/C_D$  ratio after only a few iterations and considerably outperformed the PCA-based method (Figure 8(b)) in terms of the optimization efficiency. Both dimensionality reduction models outperformed the conventional optimization method (i.e., the NURBS-based airfoil curve parameterization method) in terms of the optimization convergence rate. Figure 8(c) shows that the NURBS-based conventional optimization method had the lowest convergence rate.

## 5. Conclusion

The GAN-based dimensionality reduction method for aerodynamic shape data presented in this study accelerates the ASO process and alleviates the problem of large computational loads associated with the optimization process to some extent. However, some issues remain that require improvement or in-depth investigation. The GAN-based reduction in the dimensionality of aerodynamic shape data is only a subprocess of ASO. In addition, the training of a neural network is a global search optimization process. Hence, it is possible to use deep learning theories to implement the entire ASO process. For example, aerodynamic target constraints (e.g., the  $C_L/C_D$  ratio) can be used as labels for training neural networks. There is no one-to-one correspondence between LCs and the physical characteristics of airfoils. LCs with higher interpretability could be generated by modifying the model structure and training parameters.

## Declarations

(1) Availability of data and materials:

The airfoil dataset used in our experiments is UIUC Airfoil Coordinates Database. All data generated or analysed during the current study are available from the corresponding author on reasonable request.

(2) Competing interests: Not applicable

(3) Funding: Not applicable

(4) Authors' contributions:

Jun ZHANG: Conceptualization, Methodology and Writing - Original Draft

Wenzheng WANG: Conceptualization, Supervision and Writing - Review & Editing

Qiuyu WU: Software, Validation, Investigation and Formal analysis

## Liwei HU: Investigation, Formal analysis, Data Curation and Visualization

### (5) Acknowledgements:

Thanks to Professor. Zhonghua Han from School of Aeronautics, Northwestern Polytechnical University for providing us with technical support.

### (6) Authors' information:

Jun ZHANG was born in 1972 and is an engineer at the School of Computer Science and Engineering of the University of Electronic Science and Technology of China. He has had a long career in teaching and research in the fields of computer software, network communication, and machine learning.

### References

- [1] Viswanath A, Forrester A, Keane A. Constrained design optimization using generative topographic mapping[J]. AIAA journal, 2014, 52(5):1010-1023.
- [2] Gao Z, Wang C. Aerodynamic shape design methods for aircraft: status and trends [J]. Acta Aerodynamica Sinica, 2017, 35(4): 516-528.
- [3] Hicks R M, Murman E M, Vanderplaats G N. An assessment of airfoil design by numerical optimization[J]. , 1974
- [4] Hicks R M, Henne P A. Wing design by numerical optimization [J].Journal of Aircraft, 1978,15(7):407-412
- [5] Zhang Z, Xie J. Aerodynamic shape optimization design of low Reynolds number airfoil [J]. Energy and Energy Conservation, 2020.
- [6] Wang X, Gao Z. Aerodynamic optimization design of airfoil based on genetic algorithm [J]. Acta Aerodynamica Sinica, 2000, 18(03): 324-329.
- [7] Han Z H, Görtz S. Hierarchical kriging model for variable fidelity surrogate modeling[J].AIAA journal,2012,50(9):1885-1896.
- [8] Han Z et al. Kriging surrogate model and its application to design optimization [J]. Acta Aeronautica et Astronautica Sinica, 2016, 197-3225.
- [9] Sun M, Zhan H. Application of Kriging surrogate model for aerodynamic shape optimization of wing [J]. Acta Aerodynamica Sinica, 2011, 29(6):759-764.
- [10] Sun J, Liu G, Jiang X. Research of rotor airfoil design optimization based on the Kriging model [J]. Acta Aerodynamica Sinica, 2013, 31(4): 437-441.
- [11] Lukaczyk T W, Constantine P, Palacios F, et al. Active subspaces for shape optimization[C].10th AIAA multidisciplinary design optimization conference, 2014, 1171.
- [12] Berguin S H, Mavris D N. Dimensional design space exploration of expensive functions with access to gradient[C]. 15th AIAA/ISSMO Multidisciplinary Analysis and Optimization Conference ,2014, 2174.
- [13] S. H. Berguin, D. Rancourt, D. N. Mavris. Method to facilitate high dimensional design space exploration using computationally expensive analyses[J]. AIAA Journal, 2015, 53(12): 37523765.
- [14] Grey Z J, Constantine P G. Active subspaces of airfoil shape parameterizations[J]. AIAA Journal,2018,56(5): 2003-2017.
- [15] Viswanath A, Forrester A, Keane A. Dimension reduction for aerodynamic design optimization[J]. AIAA journal, 2011, 49(6):1256-1266.
- [16] Yasong Q, Junqiang B, Nan L, et al. Global aerodynamic design optimization based on data dimensionality reduction[J]. Chinese Journal of Aeronautics, 2018, 31(4):643-659.
- [17] Berguin S, Mavris D. Dimensionality reduction using principal component analysis in aerodynamic design[J]. AIAA Paper, 2014.
- [18] Kipf T N, Welling M. Variational graph autoencoders[J]. arXiv preprint arXiv:1611.07308,2016.
- [19] Goodfellow I J, Pouget-Abadie J, Mirza M, et al. Generative adversarial networks[J]. Advances in neural information processing systems, 2014:2672–2680.
- [20] Hennigh O. Latnet: compressing lattice boltzmann flow simulations using deep neural networks[J]. arXiv preprint arXiv:1705.09036, 2017.
- [21] Achour G, Sung W J, Pinon-Fischer O J, et al. Development of a conditional generative adversarial network for airfoil shape optimization[C]. AIAA Scitech 2020 Forum, 2020, 2261.
- [22] Chen W, Chiu K, Fuge M. Aerodynamic Design Optimization and Shape Exploration using Generative Adversarial Networks [C]. AIAA SciTech Forum, 2019.
- [23] Chen X, Duan Y, Houthoofd R, et al. Infogan: Interpretable representation learning by information maximizing generative adversarial nets[C]. 30th Conference on Neural Information Processing Systems (NIPS 2016), 2016.
- [24] Wold S, Esbensen K, Geladi P. Principal component analysis[J]. Chemometrics and intelligent laboratory systems, 1987, 2(13):37-52.
- [25] Moćkus J. On bayesian methods for seeking the extremum[C]. Optimization techniques IFIP technical conference, 1975, 400-404.
- [26] Jones D R, Schonlau M, Welch W J. Efficient global optimization of expensive blackbox functions[J]. Journal of Global optimization, 1998, 13(4): 455-492
- [27] Lepine J, Trepanier J Y, Pepin F. Wing aerodynamic design using an optimized NURBS geometrical representation[C]. 38th Aerospace Sciences Meeting and Exhibit, 2000, 669.